

MACHINIC VISIONS OF THE PLANETARY

The "Cartographic Impulse" and Its Epistemic Gains in the Process of Iteratively Mapping M87's Black Hole

Paula Muhr^{1a}¹ Institute for History of Art and Architecture, Karlsruhe Institute of Technology

Keywords: black hole, cartographic impulse, algorithmic imaging, image operativity, processuality of mapping

<https://doi.org/10.1525/001c.88163>

After the Event Horizon Telescope Collaboration released in April 2019 the first empirical images of a black hole, an astrophysical object previously thought “unseeable,” much of the public discourse has approached these images as straightforward visual depictions of a black hole. This article challenges this view by showing that the first images of a black hole went beyond merely making an invisible cosmic object visible and that the images published in April 2019 were just the first in a series of black hole images the researchers continue producing. Drawing primarily on Sybille Krämer’s concept of the cartographic impulse, the article demonstrates that the Event Horizon Telescope images are, first and foremost, epistemic tools. These epistemic tools enable researchers to actively explore various physical aspects and dynamic properties of a black hole’s immediate environment and test theoretical predictions about it, thus making this elusive environment empirically knowable. To demonstrate this, the article analyses the mapping operations that combined automated algorithmic procedures with expert human judgment and through which these images were produced, read, and interpreted. It also examines how the different Event Horizon Telescope images relate to one another, which particular epistemic functions they fulfil in the research context, under which conditions, and with which limitations, thus tracing how these images facilitate the production of new scientific knowledge about black holes.

Black holes, which were initially predicted by Einstein’s general relativity and are now thought to reside in all galaxies, are the most extraordinary physical environments in the universe. Their mass—which in the largest specimens, termed supermassive black holes, can reach billions of solar masses—is densely packed, causing an enormous gravitational pull (Goddi et al. 2019, 25–26). As a result, black holes warp the surrounding space-time, thus bending the light that passes near them and deflecting it from its straight-line trajectory, a phenomenon known as gravitational lensing. Moreover, due to its gravitational pull, a black hole traps anything that crosses its boundary, called the event horizon. While laws of physics are expected to break down inside the event horizon, general relativity and competing theories of gravity offer mathematical descriptions of processes occurring in the black holes’ immediate surroundings (Goddi et al. 2019, 26).

^a Paula Muhr is a postdoctoral researcher at the Institute for History of Art and Architecture, Karlsruhe Institute of Technology (KIT) and a visual artist. She studied visual arts, art history, theory of literature, and physics before receiving her PhD in Art and Visual History from the Humboldt University Berlin. Her interdisciplinary research is at the intersection of visual studies, image theory, media studies, science and technology studies (STS), medical humanities, and history and philosophy of science. She examines knowledge-producing functions of new imaging and visualisation technologies in natural sciences, ranging from neuroscience over medicine to black hole physics. Since 2022, she is an active member of the History Philosophy and Culture (HPC) Working Group of the Next Generation Event Horizon Telescope (ngEHT) Collaboration. She recently published her first monograph *From Photography to fMRI: Epistemic Functions of Images in Medical Research on Hysteria* (transcript, 2022; open-access).

Black holes are essentially invisible since no light can escape from within their event horizon. However, general relativity predicts that the inflowing matter—which swirls around the event horizon in a ringlike structure—heats up, turning into magnetised plasma that emits bright radiation across multiple wavelengths (Falcke, Melia, and Agol 2000). This luminous structure, called the accretion disc, is thought to power relativistic jets—beams of particles travelling near the speed of light—which black holes emit along their rotation axis. According to calculations, when observed from an infinite distance, the accretion disc of a black hole should feature a “shadow”—a dark circular region in the disc’s centre (Falcke, Melia, and Agol 2000, L14). The apparent boundary of this shadow is defined by a so-called lensed photon ring. Due to the gravitational lensing (i.e., light bending) caused by the black hole, the diameter of the shadow should appear several times larger than that of the event horizon when viewed by a distant observer.

Evidence for this prediction was delivered in April 2019, when the Event Horizon Telescope (EHT) Collaboration, an international project then gathering over two hundred scientists from twenty countries, revealed the first empirical images of M87*, a candidate supermassive black hole some fifty-five million light years away from Earth (EHTC 2019a).¹ The four initial images, published in a series of papers in the *Astrophysical Journal Letters*, were reconstructed from massive amounts of radio signal data by tailor-made imaging algorithms using machine learning techniques and show a blurry orange-yellow ring with a dark circular patch in the centre (Galison 2021) ([figure 1](#)).² One of these images circulated in the general press and social media across the globe and was widely celebrated for making an “unseeable” cosmic object visible (Dunham 2019; Strickland 2019). This characterisation is not factually incorrect, although the EHT images visualise not the black hole itself but its immediate environment—M87* is assumed to lurk inside the shadow defined by the surrounding luminous ring. However, in my view, the above characterisation unduly simplifies the EHT images by implicitly reducing them to passive visual depictions of what the black hole’s vicinity would look like if visible. This characterisation overlooks the multiple epistemic functions that the images of M87* released in 2019, and the more abstract ones that followed in the subsequent two years (Wielgus et al. 2020; EHTC 2021a, 2021b), fulfil in the context of black hole research.

1 M87* designates the candidate supermassive black hole, whereas M87 (the abbreviation of Messier 87) refers to the galaxy in which M87* is located.

2 Machine learning here is very broadly understood as “programming computers to optimize a performance criterion using example data or past experience. We have a model defined up to some parameters, and learning is the execution of a computer program to optimize the parameters of the model using the training data” (Alpaydin 2020, 3). Although strictly speaking not machine learning, the EHT imaging algorithms were developed, evaluated, mutually compared, and gradually improved by deploying large training and testing datasets that were specifically generated and curated for this purpose, a technique adopted from “machine learning communities” and not typically used in radio astronomy (Bouman 2017, 133). Moreover, as we will see later, to determine the imaging algorithms’ optimal free parameters, the EHT team relied on tailored synthetic ground truth datasets.

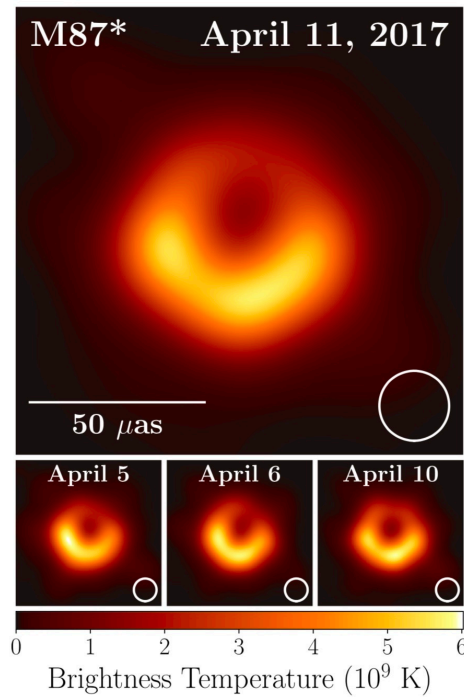


Figure 1. EHT images of M87* for four separate measurement days in April 2017 obtained by averaging three different algorithmic image reconstruction methods.

EHTC 2019a. <https://creativecommons.org/licenses/by/4.0/>.

In this article, I argue that the diverse EHT images are made and deployed by researchers as novel visual tools for actively exploring and generating new scientific knowledge about a previously unknown environment. In short, scientists working with the EHT images use them primarily as maps. A map here is understood as a digrammatically arranged visual artefact that functions as a heuristic device (Ljungberg 2016) or, more specifically, as a means of navigation (November, Camacho-Hübner, and Latour 2010) and a medium of orientation, where orientation is needed (Krämer 2011, 2015, 2018).³ Importantly, a map “is not simply a record of a terrain that has already been charted but, instead, it has the capacity to generate new fields of knowledge in either physical or mental spaces” (Ljungberg 2016, 139; see also Siegert 2011).

Approaching the EHT images as maps, in this article, I will address the following questions: Through which procedures were these images constituted as maps of a black hole? Why have the scientists produced multiple images of the same black hole, and how do these images relate to one another? If, as the German philosopher Sybille Krämer claims, “something is a map only when it is in use” (2011, 277), how do researchers deploy the EHT images as maps? Moreover, when used as maps, what kinds of insights into black holes do these images generate, and what are their epistemic limitations? To answer

³ Navigation, in turn, is understood as an “operational practice” that “continuously updates and adjusts multiple frames from viewpoints within and beyond the world” (Mende and Holert 2019, n.p.). And for Ljungberg (2016, 141), “all maps are diagrams” because a map “creates an intelligible [visual] structure by making [spatial] relations between objects visible.”

these questions, this article will draw on Krämer’s concept of the “cartographic impulse” (Krämer 2011, 276), Bruno Latour’s notion of stable inscriptions (Latour 1987, 1999), and the claim by scholars of critical cartography that mapping is always a relational and processual practice (Kitchin, Perkins, and Dodge 2011).

The Cartographic Impulse and the Processuality of Mapping

As defined by Krämer, the cartographic impulse is a knowledge-generating operation. It entails using particular kinds of images that Krämer refers to as “operative” (2018, 23). In Krämer’s use (2009, 103), operative images designate various visual inscriptions—spatially organised two-dimensional arrangements—that have a demonstrable referential relation to an external object but cannot be reduced to passive representations of that object. In representing an object, according to Krämer, operative images open spaces for examining and interacting with this object. They are, therefore, epistemic tools whose primary purpose is to be actively deployed by their human users for gaining new insights into the visualised object. Importantly, Krämer’s concept of operative images should not be confused with Harun Farocki’s more widely known use of this term. For Farocki (2004), operative images are made by machines and for machines, thus bypassing humans. By contrast, Krämer foregrounds the active role of the operative images’ human users.⁴

According to Krämer (2009), to deploy operative images as tools for epistemically exploring the visualised object, their users must know how to adequately approach and engage with such images. She thus argues that rather than merely being looked at, operative images must be read akin to texts. To read operative images, their informed users require expertise to determine the images’ salient visual features that carry the information of interest about the visualised object (Krämer 2009, 102) and that may not be evident to a nonexpert. Concurrently, informed users must know which visual features are epistemically irrelevant in a particular context and should be ignored. Hence, such targeted reading, which is context specific and consensually established among expert users, involves selectively focusing on the operative image’s epistemically salient spatial relations and configurations. It is in this sense that for Krämer (2018, 23–24), an image, when used operatively, functions as a diagram.

Having identified the operative images’ salient visual configurations, the users can then deploy these two-dimensional configurations to orientate their action in “the real space of the lifeworld” (Krämer 2011, 277). This transformation of an operative image’s virtual configurative space into a space of action is what Krämer calls the cartographic impulse. Developing this concept, Krämer

⁴ For a recently published discussion of the EHT images that explicitly draws on and expands Farocki’s concept of operative images, see Parikka (2023, 211–20). For an alternative approach to operative images that, similarly to Krämer, pays attention to the roles of human users, see Hoel (2021). Moreover, Hoel (2018) offers a pertinent overview of different media theoretical approaches to operative images.

(2011) draws on everyday uses of topographic maps (e.g., city maps and subway plans) that facilitate goal-oriented movement in actual physical spaces, thus enabling users to navigate unfamiliar terrains. By establishing an analogy between physical movements in unknown landscapes guided by topographic maps, on the one hand, and an intellectual activity in a new knowledge field supported by operative images, on the other hand, Krämer significantly expands the meaning of the cartographic impulse. It is in this broader sense, understood as an “operative principle” in “the realm of the cognitive” (Krämer 2021, 85), that I use the cartographic impulse here. Deploying this concept, I will show that, although the EHT images of M87* cannot facilitate human movement around a black hole (such as in topographic maps of terrestrial environments), these images successfully provide epistemic orientation to researchers who operatively use them to gain new insights into structural and dynamic physical features of the visualised black hole.

Krämer’s approach to maps, and operative images in general, is critical to our discussion because its focus on the operations underpinning the images’ epistemic implementations will allow us to examine how researchers work with the EHT images as finished products. However, the drawback of Krämer’s approach is that it pays little attention either to the mapmaking process—that is, the operations entailed in the image production—or to the implicit power relations inherent in the maps’ creation and application as knowledge-producing tools (Kitchin, Perkins, and Dodge 2011, 9). Since the latter aspects, as I will show later, are important when examining the EHT images’ epistemic functions, my analysis is additionally informed by critical cartography and science and technology studies. Pertinently, proponents of critical cartography have argued that, rather than considering a map as an isolated, singular representation, we must view it as part of an ongoing process of mapping, “an inscription in a constant state of re-inscription” (Kitchin, Perkins, and Dodge 2011, 21). Thus, to uncover the processual nature of maps, we should analyse them “as simultaneously being produced *and* consumed, authored *and* read, designed *and* used, serving as a representation *and* practice” (Kitchin, Perkins, and Dodge 2011, 17).

In this article, I will adopt such processual framing, coupled with the insistence that each map is always “relational and context-dependent” (Kitchin and Dodge 2007, 5). First, this will allow me not just to discuss the specificities of the EHT mapping procedure and its epistemic consequences for the resulting images but also to examine why, instead of producing a single, definitive map, the EHT team have iteratively created, read, and interpreted chains of mutually complementary maps of M87*. Second, while my primary focus will remain on examining the epistemic functions of the EHT images, this approach will also enable me to touch upon some of the images’ broader sociocultural implications. We will thus see that, when used as maps, the EHT images “produce power” (Kitchin and Dodge 2007, 332) as they reshape our understanding of the universe by reconfiguring the limits of what is knowable

to us humans. Moreover, in conclusion, I will also point out that the operative use of these images as maps with which new knowledge about black holes can be gained is restricted to a small circle of experts.

However, I will depart from the view that all maps are inherently mutable (Kitchin, Perkins, and Dodge 2011, 21). Instead, following Krämer (2011) and Bruno Latour (1987, 1999), I will suggest that the EHT images’ visual fixity is a precondition for their epistemic operativity in the scientific context. Latour has convincingly argued that to enable us to “act at a distance” in an otherwise unfamiliar terrain, a map needs to be materialised into a stable inscription that can be moved from one place to another without “distortion, corruption or decay” (1987, 223). Latour has thereby emphasised that both the map’s material stability and its referential quality—that is, its capability to provide access to the otherwise inaccessible terrain—are inextricably linked to a series of targeted manipulations that went into the map’s production. These manipulations result in a cascade of mutually aligned intermediary inscriptions, which are gradually and successively transformed into the final map (Latour 1987, 233–37; 1999, 24–79). Thus, according to Latour, the map’s material stability as a visual artefact and its knowledge-producing capability are mutually interlinked, and are both products of the long chain of transformations that underpins the map’s creation (Latour 1999, 70–72).

Yet although my analysis will draw on Latour, I will also show that, despite their stable visual forms, which facilitate the implementation of the cartographic impulse, the existing EHT images’ operative meanings continually shift with the creation and interpretation of new EHT images. Doing so will allow me to highlight how the EHT images as novel visual tools mediate the production of new scientific insights into black holes by offering new access to these astrophysical objects but by doing so under highly specific operational conditions. And as we will see, these operational conditions “are not all exclusively technical *a priori*s but involve the materiality of media in the broadest sense, including their technicality, discourse networks, cultural techniques and formations of knowledge” (Siegert 2011, 15).

My analysis is grounded in close reading of eight peer-reviewed articles the EHT team published from April 2019 to March 2021 (EHTC 2019a, 2019b, 2019c, 2019d, 2019e, 2019f, 2021a, 2021b) and an additional article from September 2020 (Wielgus et al. 2020). These articles jointly delineate the EHT team’s procedure of mapping M87*, whose following successive stages I will address: first, mapping the topography of M87*’s immediate surroundings; second, using the images to epistemically navigate the unknown astrophysical environment; and third, exploring the accretion flow’s dynamic features. By outlining and discussing the operations researchers have performed during each successive stage of this mapping, I aim to reveal the multifaceted procedural aspects that underpin the production and use of the EHT images as new and powerful knowledge-generating tools in black hole research. I will

thereby claim that examining these procedural aspects, which are rarely discussed in sufficient detail beyond the expert circles, is crucial for understanding what kinds of scientific insights these images enable, under which conditions, and with which limitations. Thus, while being a case study of the EHT’s mapping of a particular black hole, this article aims to contribute to broader discussions on how images are implicated in the production of scientific knowledge (see, e.g., Coopmans et al. 2014; Vertesi 2015).

Creating Topographic Images of M87*’s Environment

On four days in April 2017, the EHT team pointed seven mutually synchronised radio telescopes located at five geographic sites across the globe towards the compact radio source at the centre of the Messier 87 (M87) galaxy (EHTC 2019d, 5) ([figure 2](#)).⁵ The aim was to collect sufficient radio signal data to create the first spatially resolved images of that source. At that point, the nature of M87*, the radio source in the M87 galaxy, had not been settled. The bright intergalactic jet this object emits was initially observed in 1918, and M87* has been studied since (EHTC 2019e, 1). Yet the dominant hypothesis that M87* is a supermassive spinning “black hole surrounded by a geometrically thick, optically thin, disk accretion flow” (EHTC 2019e) lacked empirical evidence, which the EHT team intended to provide.

For this purpose, the EHT team conceptually and technically expanded a method called very long based interferometry (VLBI). This method has been used in astronomy since the 1960s for imaging distant radio sources by virtually connecting multiple pairs of widely spaced telescopes into arrays (Thompson, Moran, and Swenson 2017). Consisting of mutually synchronised radio telescopes arranged in a particular spatial configuration, a VLBI array operates as a single instrument, with all the telescopes simultaneously collecting radio signals emitted by the object observed. To collect sufficient data for the subsequent image reconstruction, VLBI arrays make use of the fact that Earth’s rotation during the measurement leads to changes in the configuration of the array relative to the observed astrophysical object, a technique called Earth-rotation synthesis (Thompson, Moran, and Swenson 2017, 31–34). The thus obtained radio signals are subsequently pairwise aligned to obtain interferometric data, “or Fourier components, of the radio brightness distribution on the sky” (EHTC 2019a, 2), from which a two-dimensional image of the measured radio source is computationally reconstructed.

⁵ The EHT array that was deployed in April 2017 to measure multiple astrophysical objects consisted of eight mutually synchronised telescopes (see [figure 2](#)). However, the eighth station, the South Pole Telescope (STP), was not used for observing M87* because, due to its location, it could not register radio waves emitted by M87* (EHTC 2019d, 5). Instead, in April 2017, the STP partook in the VLBI measurements of the quasar 3C 279 and SagA*, the black hole in the centre of our galaxy. Although, in the meantime, the EHT team released the reconstructed images of 3C 279 and SagA*, the discussion of these images is beyond the scope of this article due to the technical specificities of their respective image reconstructions.

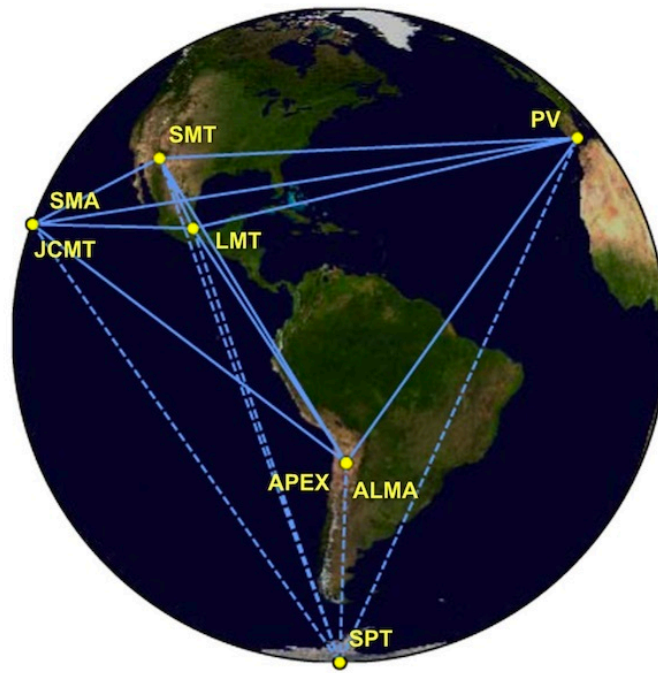


Figure 2. Map of the EHT2017 array configuration.

Solid lines connect the telescopes used for collecting radio signals from M87* in April 2017. EHTC 2019c. <https://creativecommons.org/licenses/by/4.0/>.

Notably, adapting the VLBI for the first full-scale measurement of M87* in April 2017 took more than two decades of preparation. During this period, the researchers worked on technologically upgrading their VLBI array to measure at shorter wavelengths and gradually expanding it through new telescopes to increase its resolution and sensitivity (EHTC 2019a, 2). In parallel, they performed computer simulations of general relativistic models that generated predictions about the appearance of black holes’ surroundings (Falcke, Melia, and Agol 2000). Before the April 2017 measurement, the team also developed new image reconstruction algorithms tailored to the extreme sparsity and noisiness of their future data and organised a series of “imaging challenges” to test the performance of these algorithms using synthetic training data generated from existing astronomical and everyday images (Bouman 2017; Bouman et al. 2016).⁶ Moreover, from 2009 to 2013, they conducted four test measurements of M87* that, because of the incompleteness of the EHT proto-arrays, delivered insufficient data coverage for image reconstruction (Wielgus et al. 2020, 4–5). Jointly, these operations were epistemically significant because they informed and constrained the subsequent 2017 measurement that enabled the creation of M87*’s first empirical images. Thus, following Kitchin, Perkins, and Dodge (2011), I argue that these decades-long preparatory operations were intrinsic to mapping M87*.

⁶ During such “imaging challenges,” different teams of researchers used different algorithms to reconstruct images from the same set of synthetic data and subsequently compared the reconstruction accuracies of the different algorithms (Bouman 2017, 135–84).

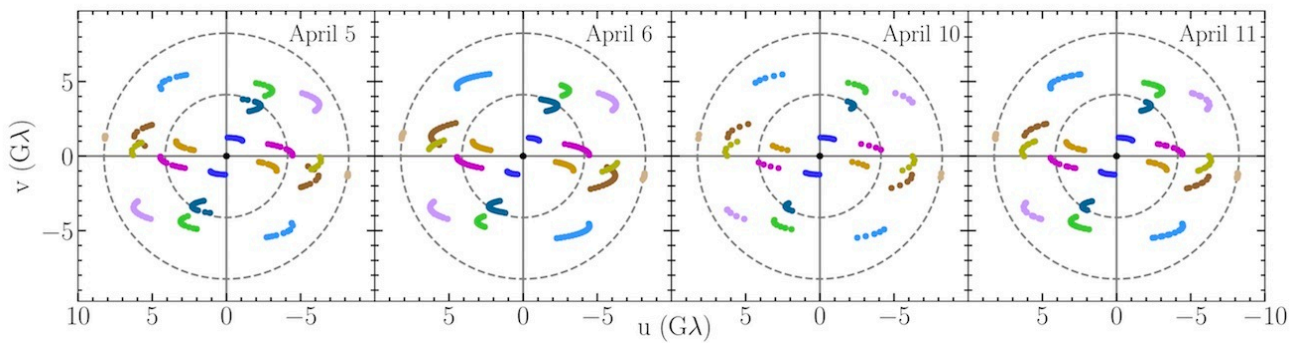


Figure 3. EHT baseline coverage (Fourier components) of M87* for each measurement day in April 2017.

EHTC 2019d. <https://creativecommons.org/licenses/by/4.0/>.

However, even after completing their 2017 measurement, the team were far removed from obtaining a spatially resolved two-dimensional image of M87* from their nonvisual radio signal data. Thus, at this point, they entered the subsequent phases of mapping, which jointly lasted almost two years. These entailed, first, the extensive data processing (consisting of correlation and calibration); and second, the multistage image reconstruction (EHTC, 2019a, 2019b, 2019c, 2019d; Muhr 2024). Working under the hypothesis that M87* is a dynamic object whose morphology changes across days but remains stable during a single-night measurement, the team decided to reconstruct a separate image for each measurement day. But the calibrated interferometric data (i.e., Fourier components), which they obtained through the pairwise correlation of radio signals using two specialised supercomputers and three tailored data reduction pipelines, were still very noisy (EHTC 2019c). Also, despite the deployment of the Earth-rotation synthesis, the resulting Fourier components were extremely fragmentary due to the small number of telescopes in the array (figure 3). This meant that by using specialised algorithms to computationally fill in the missing data, the EHT team could reconstruct an infinite number of images from the sparse EHT2017 dataset (EHTC 2019d). Simply put, the challenge the team faced was how to translate their sparse, noisy data into images that were not mere artefacts of the algorithmic reconstruction but had a verifiable referential relationship to M87*. This was crucial because only such images could be justifiably used by the researchers to navigate the M87*'s unknown environment and thus “act [on it] at a distance” (Latour 1987, 223).

Elsewhere, I have argued that to meet this challenge, the EHT team developed a custom-built image reconstruction procedure that comprised an entire network of interrelated algorithmic and discursive operations (Muhr 2024). Drawing on Latour (1999), I have shown that these operations were organised into successive stages of a complex, multibranching chain of transformations that gradually translated the sparse EHT2017 signal data into final images via a long cascade of mutually aligned intermediary inscriptions (figure 4). I have also shown that each stage of this multibranching chain entailed a parallel

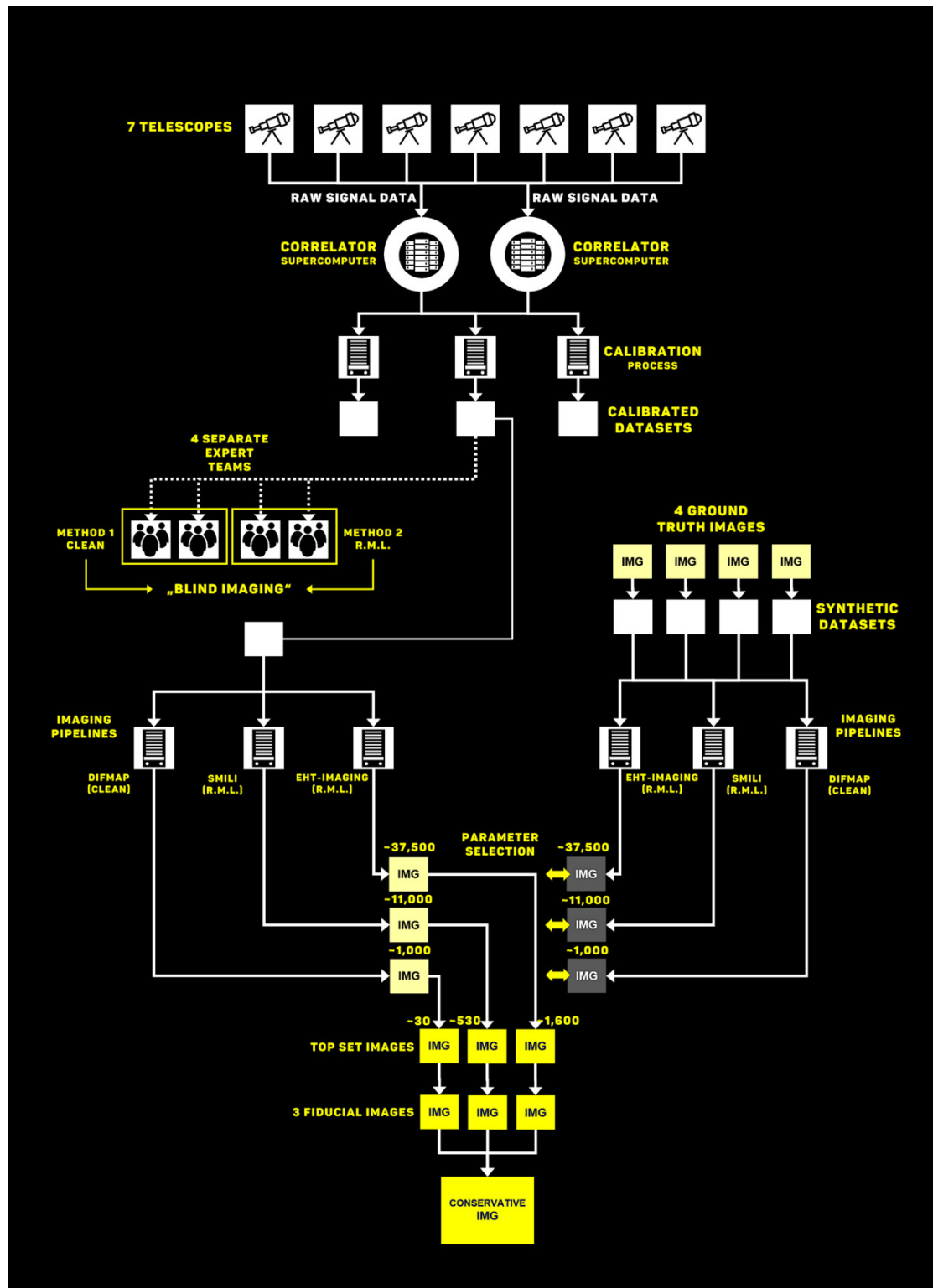


Figure 4. Custom-built multibranch chain of transformations that underpinned the production of the total intensity EHT images of M87* for each measurement day in April 2017.

Image concept: Paula Muhr. Graphic design: Gerold Muhr.

implementation of different methodological approaches and statistical models whose independently obtained algorithmic results mutually reinforced each other's empirical authenticity and validity (Muhr 2024).

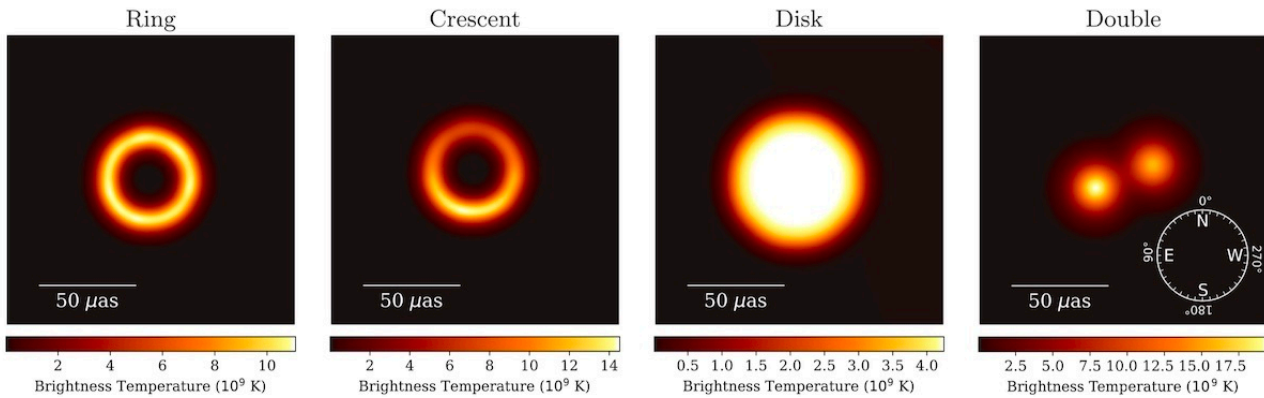


Figure 5. Four simple geometric models used as ground truth images for determining the optimal imaging parameters of the three EHT image reconstruction pipelines.

EHTC 2019d. <https://creativecommons.org/licenses/by/4.0/>.

While the details of this procedure are beyond the scope of this article, relevant to our current discussion is that the EHT image reconstruction combined state-of-the-art algorithms developed specifically for this purpose with strategically implemented expert human judgment (Muhr 2024). For example, in the key stage of the image reconstruction, the researchers chose to use not one but three scripted image reconstruction pipelines (DIFMAP, SMILI, and eht-imaging), whose optimal free parameters they selected by using the specifically for this purpose generated synthetic data (EHTC 2019d; Muhr, Forthcoming).⁷ These three mutually independent pipelines were informed by two different statistical data modelling approaches (i.e., inverse and forward modelling), and each pipeline used a different sequence of algorithmic operations that were performed in iterative loops to gradually build the images from the sparse and noisy EHT data (EHTC 2019d, 12–14).⁸ In addition to designing the pipelines, the researchers also made decisions on which and how many predefined abstract geometric models to use as ground truth images to test and evaluate the performance of their algorithmic pipelines across a wide range of imaging parameters (EHTC 2019d, 14–18) (figure 5).⁹ Moreover, to determine the single most faithful image reconstruction for each pipeline, the researchers defined a set of quantitative fidelity criteria (EHTC 2019d, 14–17).

⁷ For a discussion of the preceding stage of image reconstruction from the EHT data, referred to as “blind imaging,” in which the algorithms were not used in an automated manner, see Muhr (2024). During this stage, four teams of experts, working independently of one another, relied on their collective expert judgement to determine the optimal combination of parameters for the algorithmic reconstruction of images from the EHT data (EHTC 2019d, 9). For the role of “blind imaging” during the aforementioned “imaging challenges,” which were organised for testing and developing new algorithms for the EHT image reconstruction even before the actual measurement took place, see Bouman (2017, 135–84) and Skulberg (2021, 147–86).

⁸ The DIFMAP pipeline was a scripted version of the CLEAN algorithm, which is based on inverse modelling and has been used in VLBI since the 1970s. The other two pipelines implemented algorithms specifically developed by the EHT team using a forward-modelling method called Regularised Maximum Likelihood (RLM). The RLM method “starts with an image—say, a fuzzy blob—and uses the observational data to modify this starting guess until it finds an image that looks like an astronomical picture and has a high probability of producing the measurements we observed” (Bouman 2020, 29).

⁹ For a detailed discussion of this process from a media studies perspective, see Muhr (Forthcoming). For a more general discussion of the role of ground truth images in the development of machine learning algorithms, see Jatón (2021).

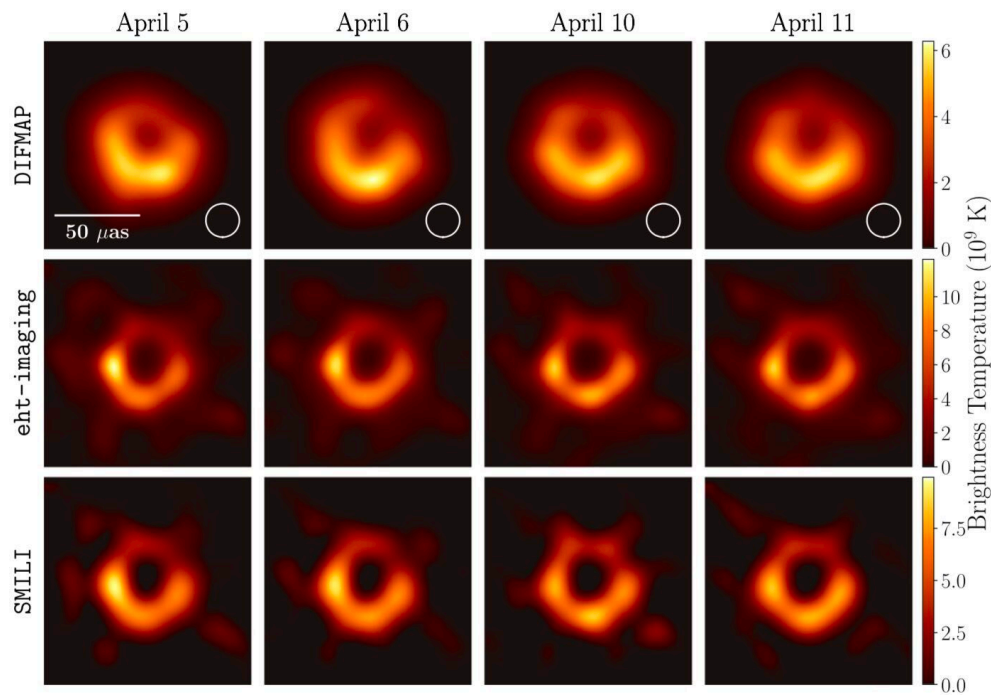


Figure 6. Fiducial images of M87* reconstructed by three independent algorithmic pipelines for four measurement days in April 2017.

EHTC 2019d. <https://creativecommons.org/licenses/by/4.0/>.

Separately, each algorithmic pipeline produced thousands of possible image reconstructions from each measurement day’s dataset using different imaging parameters. Applying the predefined quantitative fidelity criteria, from this abundance of images, through a two-stage procedure, the researchers identified one optimal image for each algorithmic pipeline and each measurement day.¹⁰ Each such image was deemed to be the most faithful and, therefore, the most trustworthy—that is, “fiducial”—reconstruction of the sparse EHT data with the respective algorithmic pipeline (EHTC 2019d, 18). Through this selection, the researchers determined twelve fiducial topographic images of M87*’s immediate environment (figure 6). These so-called total intensity images visualise the algorithmically reconstructed distribution of M87*’s brightness intensity in the sky on the four nights in April 2017. Notably, through the telescopes’ configuration and Earth’s rotation during the measurement and the subsequent correlation performed during data processing, Earth’s relative position and geometry were inscribed into the data (EHTC 2019b, 2019c), informing the resulting images’ configurative space. Therefore, instead of an Apollonian “view from nowhere” (Krämer 2015, 2002), which is dominant in terrestrial maps, the EHT images show M87* viewed from the position of Earth, a point to which I will return when discussing the uses of these images.¹¹

¹⁰ First, the researchers narrowed down their choice to what they designated as the “Top Set” parameters that were deemed to produce “acceptable” image reconstructions for each pipeline, and then from each “Top Set” they determined the single “best-performing” parameter combination for each pipeline (EHTC 2019d, 14).

¹¹ The construction of the EHT images’ viewpoint is discussed in detail in Skulberg (2021).

Although sufficiently similar, the twelve fiducial images were not identical due to the different reconstruction methods and the algorithms’ disparate resolutions. To minimise these differences, the team averaged the three fiducial images from each measurement day after blurring them to the EHT array’s nominal resolution. In doing so, they obtained the “conservative” images of M87*’s immediate vicinity (EHTC 2019d, 21) (see [figure 1](#)). In these images, idiosyncratic visual details and statistical uncertainties stemming from each reconstruction method were attenuated through the operation of averaging. It should be noted that the twelve fiducial and the four pipeline-averaged total intensity images jointly comprise the “primary” EHT images of M87* (EHTC 2019d, 2). Whereas the fiducial images disclose how the statistically less certain visual details vary across the reconstruction methods, the pipeline-averaged images display the reconstructed visual structures that are shared by all methods. To a nonexpert, such differences between the fiducial and the pipeline-averaged images may seem inconsequential since they are not entirely discernible through mere visual inspection of the images. To fully discern these differences, the images need to be submitted to a systematic quantitative comparison. Yet, as I will show later, the fact that the fiducial and the pipeline-averaged images encode the information about M87* with different levels of statistical uncertainty influences how these images have been used epistemically in the research context.

Overall, this section has shown that through a protracted, multistage process involving automated algorithmic operations and expert human judgement, the EHT team stabilised their imaging results in fixed visual forms (Latour 1999, 29). They thus created the first empirical images that mapped a black hole’s immediate environment by translating it into a two-dimensional “configurative space” characterised by “topographical order” (Krämer 2011, 277). As detailed above, this configurative space retained a referential relationship to the distant physical environment by virtue of being a sufficiently faithful reconstruction of the sparse nonvisual measurement data according to the predefined quantitative fidelity criteria (see also Muhr 2024). Materialised in the form of stable visual artefacts (i.e., inscriptions) that could be stored, transported back and forth, measured, and inspected without being distorted through such interactions (Latour 1987, 223),¹² this configurative space opened up new access to the otherwise inaccessible, distant environment.

Importantly, the thus reconstructed visual arrangements were not passive depictions of the black hole’s environment. Instead, as we have seen, the images’ configurative space was created through the alignment of diverse operations, including decades-long conceptual and technical preparations, multiple test measurements, acquisition of nonvisual data, extensive data

¹² Whereas Latour designates such inscriptions as immutable mobiles (1987, 227), I prefer to refer to them as stable since in algorithmic imaging, visual artefacts are not entirely immutable.

processing, use of ground truth images, and the parallelised algorithmic image reconstruction. Hence, the initial EHT images of M87* and the far-off galactic territory they refer to were mutually co-constituted through these mapping operations. In short, far from simply reflecting it, “mapping activates territory” (Kitchin, Perkins, and Dodge 2011, 18) through the process of its mediation (see also Siegert 2011). This, in turn, means that by forging a highly mediated access to M87*’s otherwise inaccessible environment, the EHT images did much more than merely make it visible. Instead, they effectively transformed M87*’s unknown environment into an explorable and potentially knowable territory. Yet, once they were produced as stable visual artefacts, how could these images be deployed operatively to generate new insights into M87*? Or to put it differently, through which context-specific practice were the EHT images effectively “enacted” as maps (Kitchin and Dodge 2007, 335)? This is the question we now turn to.

The Cartographic Impulse: Using Images as Tools of Epistemic Exploration

So far, I have shown how the researchers produced the configurative space of their initial topographic images. Had these images been intended to serve as mere descriptive illustrations that made M87*’s surroundings visible, the researchers might have stopped at that. Namely, what is evident even at a cursory glance is that all the primary EHT images of M87* consistently show a blurry bright ring with a dark central patch. Since this visual structure matches the predictions of general relativity about how a black hole’s environment should appear to a distant observer, nonexperts might presume that by creating these images, the team provided empirical evidence that M87* is a black hole. However, such nonexperts would reduce the EHT images to “structural pictures” (Krämer 2011, 277), or, in other words, passive visual depictions of the black hole. Contrary to this, the researchers approached the EHT images as maps, transforming their figurative space into a space of epistemic action, thus using these images as tools that support reasoning and reflection. In the following, I will trace and discuss the operations that facilitated this transformation.

To begin with, through targeted reading of the images, the team selectively isolated only four visual features shared by all images as epistemically salient. In doing so, they effectively declared all other visual details irrelevant for their epistemic purposes. The select salient features included “the ring-like geometry,” the peak brightness, “the total flux density” (i.e., total brightness), and the ring being “brighter in the south than the north” (EHTC 2019e, 2–3). Notably, the latter feature indicates that the team approached the images as maps, since their positioning within the images’ configurative space was defined by the cardinal (compass) directions: north, south, east, and west. This attribution of the cartographic conventions already operatively transforms these images into maps. It is worth pointing out that the team deployed the cardinal directions as they are used in celestial mapping, where the directions of

east and west are reversed relative to Earth—“north is up and east is to the left” (EHTC 2019a, 5). In celestial maps (Macrobert 2017), and the EHT images, this reversal of the cardinal directions is motivated by a different viewpoint that these maps embody compared to terrestrial maps. Whereas terrestrial maps show surfaces on Earth viewed from above, celestial maps and the EHT images show the astrophysical objects viewed from Earth.

But the ascription of the cardinal directions was by far not the only operation that transformed the EHT images into maps. What even more forcefully made them into maps was how the researchers used the images’ salient visual features to “act at a distance” (Latour 1987, 223) on the visualised astrophysical object by making inferences about this object’s physical characteristics. To this end, after they identified the images’ salient visual features listed above, the researchers turned to the quantification and interpretation of these features. For example, by measuring the images’ peak and total brightness, the team inferred multiple physical properties of M87*’s accretion disc, such as the temperature and density of the electrons comprising the swirling plasma (EHTC 2019e, 2–3). Yet for the team, the images’ most salient figurative feature was the reconstructed ring’s morphology. To specify this feature, the team measured the ring’s mean diameter, width, degree of circularity, and orientation angle (the angular position of the brightest region relative to the north) across the EHT images (EHTC 2019f, 18–20) ([figure 7](#)). They also measured the relative differences in the mean brightness between the ring’s interior and rim to evaluate the images’ central brightness depression. Notably, during these analyses, the researchers used the fiducial and not the pipeline-averaged images. I suggest this is because the fiducial images allowed the researchers not just to quantify the mean visual features of interest but also to assess the features’ variance across the different reconstruction methods. In other words, using the fiducial images, the researchers could estimate the statistical uncertainty of their quantitative empirical findings and thus evaluate the findings’ reliability.

But let us return to discussing the insights that these quantitative analyses generated. The measurements of the relative differences in the mean brightness revealed that the brightness in the ring’s interior was more than ten times lower than on the edges. This finding was epistemically significant because the high contrast ratio indicated that the “central flux depression [in the images] is the result of photons captured by the black hole: the black hole shadow” (EHTC 2019f, 20). Next, using elaborate computational methods, the researchers determined the size of the ring in the images. This, too, was important because by establishing that the mean ring diameter across the reconstructed images was $\sim 42 \pm 3 \mu\text{as}$ (microarcseconds), the researchers effectively constrained the size of the hypothesised black hole shadow as seen from Earth. Crucially, they argued that it was this particular measurement that provided implicit “evidence for the existence of event horizons” (EHTC 2019f, 22). Moreover, the researchers determined that the peak brightness distribution in each image was circular

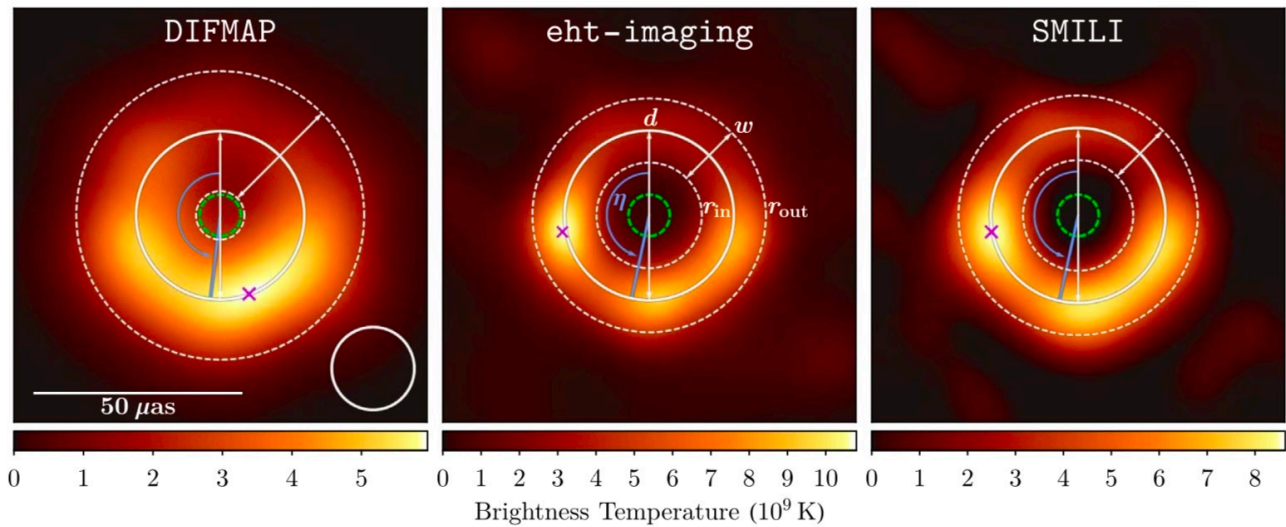


Figure 7. Schematic visualisation of the estimated ring properties overlaid on the April 11 fiducial images from each imaging pipeline.

EHTC 2019d. <https://creativecommons.org/licenses/by/4.0/>.

with a deviation from circularity below 10% (EHTC 2019a, 8). Since, according to general relativity, shadows of Kerr black holes are “nearly circular with a maximum asymmetry of 10%” (EHTC 2019f, 23), the latter result supported the conjecture that M87* is a black hole whose space-time is described by the Kerr metric and thus uniquely characterised by two parameters—mass and spin.

As the sequence of operation delineated above demonstrates, by quantifying the EHT images’ salient visual features and comparing them to theoretical predictions, the researchers actively explored and epistemically orientated themselves in a previously unfamiliar territory. Using such measurements allowed them to make inferences about the nature and structure of M87*’s immediate environment as well as to test whether the theoretical predictions of general relativity matched the salient visual features of their empirical images. It is, therefore, by performing such targeted quantitative analyses that the researchers fully activated the operative potential of the EHT images, transforming the images’ visual features into “a real space of activity” (Krämer 2011, 277).

However, through quantification alone, the team could neither infer astrophysical explanations for the salient morphological features of their reconstructed images nor use these features to estimate M87*’s physical properties, such as its mass and spin. This was because, even if assuming that M87* is a Kerr black hole, radically different physical scenarios of dynamic processes governing the behaviour of its accretion flow and the jet could have resulted in the same image morphology (EHTC 2019f, 2). To constrain the images’ interpretative ambiguity and test if M87* is indeed a Kerr black hole,

in the next step, the researchers resorted to comparing their empirical EHT images to images of idealised Kerr black holes derived from general relativistic models, a process to whose analysis we will now turn.¹³

To be able to perform the intended comparisons, the researchers first had to employ a multistep algorithmic procedure to construct an extensive library of synthetic images from general relativistic magnetohydrodynamic (GRMHD) simulations using a supercomputer. These highly sophisticated numerical simulations model the dynamic properties of a black hole’s accretion flow and jet by treating the relativistic magnetised “plasma as an ideal fluid governed by equations that encode conservation laws for particle number, momentum, and energy” (EHTC 2019e, 15; see also Mizuno 2022). In short, the complex physical processes that are presumed to take place in a black hole’s immediate environment are approximately modelled through a combination of mathematical equations.¹⁴

First, using four different codes to numerically solve the GRMHD equations that describe magnetised accretion flows orbiting an ideal Kerr black hole, the team generated forty-three three-dimensional time-dependent simulations (EHTC 2019e, 4). These simulations modelled “a wide range of black hole spins as well as initial magnetic field geometries and fluxes” that control “the structure of the accretion flow near the black hole” (EHTC 2019f, 14). Overall, the simulations were either SANE (Standard and Normal Evolution) models with low magnetic accretion flows or MAD (Magnetically Arrested Disk) models with strong magnetic fields. Next, to generate synthetic images from these dynamic three-dimensional simulations, the researchers had to specify multiple astrophysical parameters, including different properties of the accreting plasma, the black hole mass, distance to the observer on Earth, and the viewing inclination (EHTC 2019e, 4–7). By varying these parameters, the researchers simulated more than four hundred and twenty different physical scenarios. Finally, using three different general relativistic ray-tracing codes, they produced two-dimensional snapshots that captured different stages in each GRMHD simulation’s temporal evolution (EHTC 2019a, 6).

The above description, although highly simplified, makes it evident that the process of generating the GRMHD snapshots not only consisted of a long cascade of algorithmic transformations but also required the researchers to make multiple interpretational decisions, such as setting the physical parameters or choosing which and how many models to generate. As the

13 In line with the approach proposed by Epple and Erhart (2020, 17), comparison here is understood not as a neutral “instrument or tool, be it cognitive, socially or scientifically,” but as “a ‘relating’ activity” that “puts differences and similarities evenly in perspective.” Defined in such operative terms, comparing is, first and foremost, “a social and historical practice [that] is always bound up with actors and agencies that perform the comparisons and connect them with their purposes and possible outcomes—intended or not.” Hence, in the following, my analysis will focus on charting not just which comparisons the EHT team carried out but also how and for which particular epistemic purposes.

14 Concerning the EHT team’s decision on which approximations to use in their models for the sake of computational feasibility and the consequences of this decision on the interpretability of the EHT images, see EHTC (2019e, 15–18). For a more general discussion of the epistemic roles of computer simulations in scientific research on the example of high energy physics, see Morrison (2015).

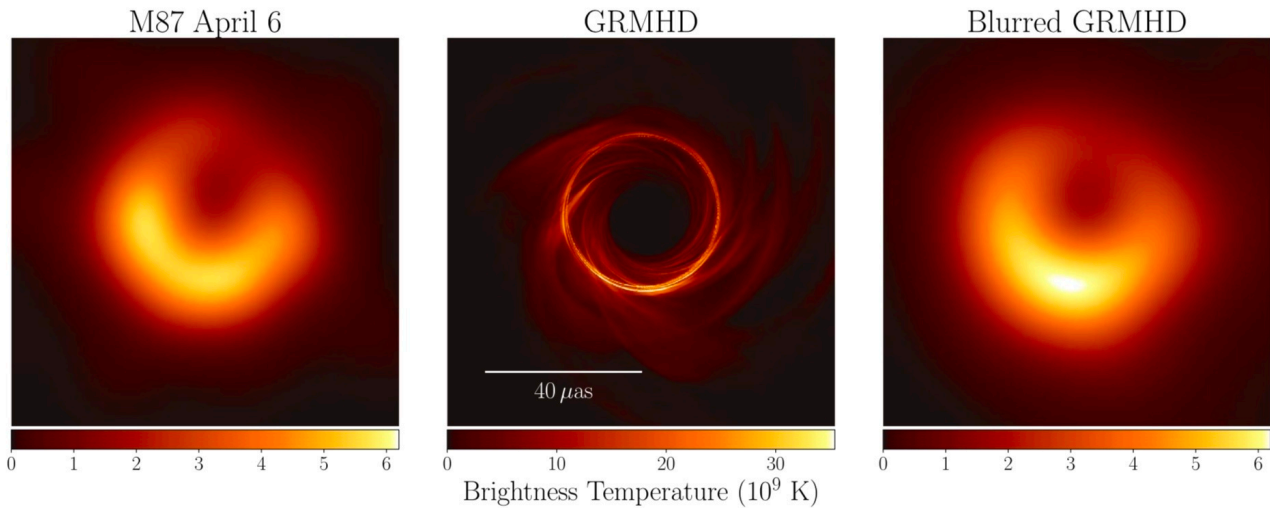


Figure 8. Comparison of a pipeline-averaged EHT image (*left*) with a full-resolution (*centre*) and a blurred (*right*) snapshot of a GRMHD simulation.

EHTC 2019e. <https://creativecommons.org/licenses/by/4.0/>.

output of this time-consuming and computationally expensive process, the resulting image library contained approximately sixty-two thousand GRMHD snapshots that could be compared to the EHT images of M87*. As I will show in the following, the comparison with these GRMHD snapshots guided the further implementation of the cartographic impulse, thus informing the kinds of insights that the researchers could derive from the EHT images.

Since they had a considerably higher resolution than the EHT images, the GRMHD snapshots showed details in the modelled accretion flow that the EHT2017 array could not resolve. A direct visual comparison between a GRMHD snapshot and an EHT image thus brought into relief the limited resolution of the latter image. But after blurring a GRMHD snapshot of an ideal Kerr black hole to the EHT resolution and placing it next to M87*'s pipeline-averaged image for 6 April 2017, the team demonstrated that the two images are strikingly similar ([figure 8](#)). The implication of this rhetorically highly effective visual ordering of the empirical and the theoretically modelled images was that they all visualised the same type of object—that is, Kerr black holes. Yet the potential weakness of this comparison was that the visual similarity might have been the artefact of blurring applied to the GRMHD snapshot.

Hence, the researchers went a step further. They selected three GRMHD snapshots of ideal Kerr black holes with different spin and accretion flow parameters (EHTC 2019a, 7). These GRMHD snapshots were specifically chosen because, although they each modelled very different physical scenarios, all the snapshots fitted equally well the interferometric data from 11 April 2017 (EHTC 2019a, 7). From each snapshot, the team computed a separate simulated interferometric dataset with the same sparseness and noise profile as the EHT2017 data. Deploying the algorithmic pipeline developed for their

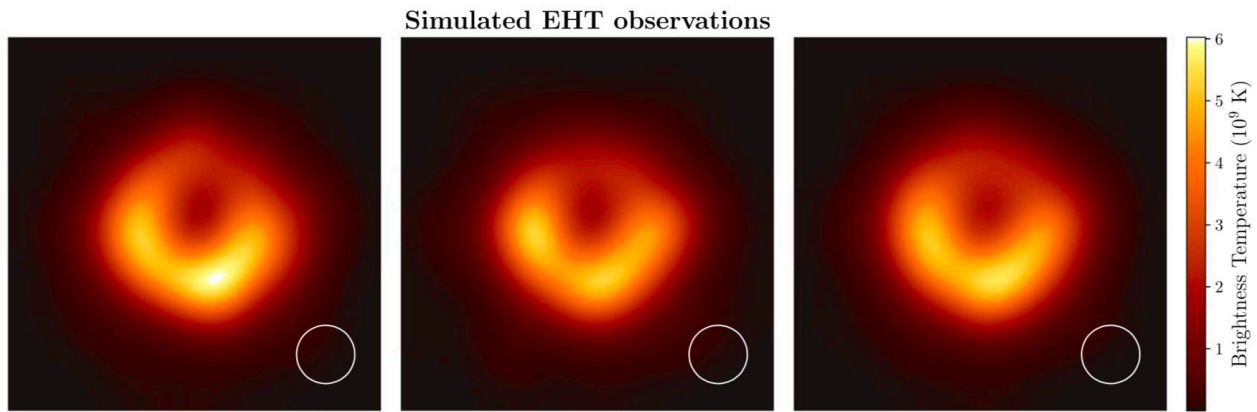


Figure 9. Pipeline-averaged images reconstructed from the simulated data derived from GRMHD simulations.

EHTC 2019a. <https://creativecommons.org/licenses/by/4.0/>.

EHT2017 dataset, the researchers then reconstructed pipeline-averaged images from the simulated GRMHD datasets (EHTC 2019a, 6). The purpose of this elaborate procedure was to enable another visual comparison that was not constrained by the need to blur the GRMHD snapshots. This second comparison revealed that the pipeline-averaged synthetic images reconstructed from the simulated GRMHD datasets (figure 9) are visually remarkably similar to the pipeline-averaged image reconstructed from the EHT2017 dataset for April 11, 2017 (see figure 1). The thus established visual similarity between the EHT image of M87* and the images reconstructed from the simulated data that modelled different variations of Kerr black holes further reinforced the conjecture that M87* is a Kerr black hole.

Thus, besides the quantitative analyses discussed above, the team also deployed targeted multilayered visual comparisons to support their conjecture about the nature of M87*. There is one aspect of these analyses that I would like to emphasise. While the team used the fiducial EHT images during their quantitative analyses to infer M87*'s physical features, they employed the pipeline-averaged images for the purely qualitative visual comparisons. As we have seen, the latter comparisons aimed to demonstrate that the empirical pipeline-averaged and the theoretically modelled images of Kerr black holes were visually equivalent and, therefore, visualise the same type of object. This was achieved by establishing among these image relations of similarity that are perceptible to the naked eye. By contrast, during quantitative analyses, the fiducial images were submitted to measurement procedures performed by algorithms. It can, therefore, be argued that the different primary EHT images fulfilled distinctly different operative functions during the mapping procedure.

But whereas the visual comparisons bolstered the hypothesis that M87* is a Kerr black hole, there remained too many radically different physical scenarios modelled through the GRMHD simulations that could have explained the EHT images' structural features. To narrow down the viable physical scenarios, the researchers turned to quantifying the similarities between the various

simulated models in their image library and their empirical images, aiming to eliminate those models that did not match the EHT data. For this purpose, they algorithmically fitted the GRMHD snapshots directly to the EHT2017 interferometric data using two independent pipelines (GENA and THEMIS) (EHTC 2019e, 7–8). Notably, this procedure of algorithmic fitting clearly resonates with Krämer’s (2009) previously mentioned claim that operative images are not meant to be looked at but instead need to be read, in this case by algorithms. However, this quantitative comparison allowed the team to reject only a group of MAD but none of the SANE models (EHTC 2019e, 10), thus leaving the theoretical interpretation of the EHT images still open-ended, with too many different models remaining as possible interpretative options. It is thereby important to point out that, by its very logic, this comparative interpretational strategy had one crucial limitation—only those physical scenarios that were explicitly modelled in GRMHD snapshots could be tested for match or mismatch with the EHT images and thus either accepted or eliminated as potentially viable physical explanations.

Finally, to eliminate further theoretical models, the researchers compared the simulated snapshots to data from non-EHT measurements of M87*’s physical properties, such as the estimated minimum jet power. But despite these additional constraints, which allowed the team to exclude most but not all of the SANE models (EHTC 2019e, 15), many GRMHD snapshots still exhibited morphologies similar to the EHT2017 images. Circumventing this potentially problematic interpretational ambiguity, the team finally settled on the conjecture that the EHT images’ salient visual features were “controlled mainly by gravitational lensing and the spacetime geometry, rather than details of the plasma physics” (EHTC 2019e, 18). Moreover, drawing on the comparison with the GRMHD simulations, the researchers posited that the ringlike structure in the EHT2017 images represented the photon ring, “the observational manifestation” of photons that repeatedly pass close to the unstable circular orbit near the event horizon before reaching Earth (EHTC 2019e, 2).

This interpretation had two important epistemic consequences as it allowed the researchers to derive additional empirical information from the EHT images and, in doing so, to further explore M87*’s environment. First, according to general relativity, the photon ring’s radius and brightness asymmetry depend on the black hole mass and spin (EHTC 2019e, 1). Comparing the EHT images to GRMHD simulations with similar north-south brightness asymmetry, the researchers identified the orientation of M87*’s rotation. They thus inferred that M87*’s spin axis “is aligned with the large-scale jet” and “pointing away from Earth” (EHTC 2019e, 8).¹⁵ Moreover, combining this insight with the previous estimation that the angle between

15 The jet is not visible in the EHT images, presumably due to the measurement’s limited resolution (EHTC 2019d, 20).

the jet and the line of sight from Earth was 17° , the researchers deduced that M87*’s accretion disc rotates clockwise from our perspective (EHTC 2019a, 6). This, in turn, permitted them to attribute the north-south brightness asymmetry in the EHT images to relativistic Doppler beaming—the ring’s bottom part is moving towards Earth and thus looks brighter, whereas the upper part appears dimmer because it is moving away from us (EHTC 2019e, 18).

Second, since according to general relativity, the black hole’s mass is located within the photon ring whose size is proportional to this mass, the researchers could use the EHT images to quantitatively assess M87*’s physical properties. During a computationally complex calibration procedure that relied on the parallel deployment of three independent algorithmic pipelines (THEMIS, dynesty, and GENA), the team used GRMHD simulations to convert the ring’s diameter in the EHT images into the black hole angular gravitational radius.¹⁶ The thus obtained value— $3.8 \pm 0.4 \mu\text{as}$ —denotes the inferred size of the photon ring in the sky from Earth’s viewpoint (EHTC 2019f, 12). Finally, adopting the prior measurement of the distance between M87* and Earth, the team used the photon ring size to estimate M87*’s mass to about 6.5 billion solar masses, which was consistent with the earlier stellar dynamics measurements (EHTC 2019f, 21–22). It is worth noting that, at this stage, the fact that the EHT images show M87* from the perspective of Earth had an important role in the images’ interpretation. As we have seen, the prior measurement of the distance between M87* and Earth, as well as the inclination angle between M87*’s jet and the line of sight from Earth were necessary for estimating the black hole’s physical characteristics based on the images’ structural features.

In sum, this section has traced how the researchers interacted with the initial images of M87* to implement the cartographic impulse. As we have seen, it was by translating the images’ two-dimensional figurative space into a space of targeted epistemic operations that they actively explored M87*’s surroundings. The operations underpinning this exploration included the selective reading and quantification of the images’ visual features, qualitative and quantitative comparisons to simulated images derived from theoretical models, and interpretation that required integrating prior non-EHT measurements. Through such operations, the team deployed the images to infer M87*’s nature and morphology, draw conclusions about the underlying astrophysical processes, and estimate the imaged object’s physical properties, all the while testing the theoretical predictions of general relativity.

¹⁶ To verify the robustness of their calibration, the researchers additionally used the same pipelines to fit simple geometric ringlike structures to the data and also measured the ring diameter directly in the reconstructed EHT2017 images (EHTC 2019f, 6–20).

Importantly, I have revealed how the epistemic efficacy of the EHT images as maps of M87* hinged on their embeddedness into the interpretative framework comprising the mathematical predictions of general relativity, computer-generated simulations of ideal black holes, and non-EHT measurements. I have also shown that in order to take place, this interpretative embedding, in turn, requires a complex network of technical and technological operations, including the parallel deployment of multiple state-of-the-art codes and algorithmic pipelines, and the use of supercomputers. It equally requires researchers’ expert decisions on which and how many comparisons to make, and which algorithms to use, as well as which theoretical approximations of hypothesised physical scenarios to model and which to neglect in their computationally expensive simulations. All these expert decisions and technical conditions are highly epistemically significant as they not only facilitate the unfolding of the cartographic impulse but also, at the same time, define the operative limits to the kinds of scientific insights that can be gained through active, explorative engagement with the EHT images. After all, as emphasised previously, only those theoretical assumptions that were explicitly modelled in tailor-made simulations and then algorithmically compared to the EHT images could be tested as viable physical explanations of the EHT images.

It is, therefore, no exaggeration to claim that when isolated from its carefully constructed interpretative framework, the EHT images become reduced to blurry pictures with no self-evident meaning. But embedded into this framework by expert users who know which visual features to focus on as salient and how to interpret them, these images function as powerful epistemic tools for navigating an unknown territory, generating new empirical insights, and testing current theoretical descriptions of black holes. As discussed above, this embedding does not happen in a single step but requires a long sequence of step-by-step operations that gradually constrain the images’ initial interpretative ambiguity. However, as we are about to see, even when used expertly, the initial EHT images had some significant epistemic limitations, which the researchers aimed to circumvent through iterative mapping of M87* that entailed generating and interpreting new images.

Exploring the Dynamic Features of M87*’s Accretion Flow

While the initial EHT images—when used as maps—enabled the researchers to probe and quantify multiple aspects of M87*’s territory, they also left many questions about this cosmic object unanswered, even opening new ones. First, despite the overall visual consistency among the images reconstructed for the four measurement days, there were some variations in the ring morphology across the days. These variations may have been measurement or image reconstruction artefacts. Conversely, they may have been caused by the temporal evolution of M87*’s accretion flow, which, based on the GRMHD simulations, was expected to occur on “timescales of up to a few weeks” (Wielgus et al. 2020, 3). However, because the measurement spanned a single week, by analysing the EHT2017 images, the researchers could not determine

which of the reconstructed ring’s morphological features were permanent and which varied over time. Second, it remained unclear if the reconstructed “ring emission is produced by plasma that is inflowing (in a thick accretion flow), outflowing (at the jet base or in a wind), or both,” and which magnetic field structure governed the plasma flow (EHTC 2021a, 1). To address the first question, the researchers created a set of abstract geometric images of M87* using their pre-2017 test data. To address the second question, they applied a different image reconstruction approach to the 2017 datasets to compute polarimetric images of M87*. These new images, I will argue, served to extend the researchers’ cartographic impulse by allowing them to probe the M87*’s dynamic features in an “‘unfolding action’ of mapping” (Kitchin and Dodge 2007, 342).

As mentioned earlier, in 2009, 2011, 2012, and 2013, the EHT team conducted test measurements with the still incomplete prototype VLBI arrays, obtaining interferometric datasets with insufficient baseline coverage to reconstruct spatially resolved images. However, in 2020, Wielgus et al. revisited these archival datasets, conjecturing that these contained information about the temporal evolution of M87*’s environment. To extract this information, instead of reconstructing spatially resolved images, it sufficed to model M87* using simple geometric figures. Before 2019 such modelling could not be performed unambiguously because different geometric figures fitted the proto-EHT data, leaving the researchers “unable to confidently select a preferred model” (Wielgus et al. 2020, 7). But Wielgus et al. argued that the morphology of the EHT images published in 2019 justified their decision to use a ring with asymmetric brightness as their geometric model. Importantly, this means that the EHT2017 images provided the necessary precondition for creating the geometric images that mapped the temporal variability in M87*’s morphology from 2009 to 2017.

To avoid overdetermining and thus unduly biasing their results, the researchers deployed two different models: a ring of varying thickness and an infinitesimally thin ring blurred to the EHT2017 array’s resolution (Wielgus et al. 2020, 8). Using the THEMIS algorithmic pipeline, which had been previously developed and deployed for analysing the EHT2017 images, Wielgus et al. fitted these models to the four proto-EHT datasets and two EHT2017 datasets from 6 and 11 April. But before they performed the fitting, the researchers tested the pipeline’s performance on the synthetic data derived from two GRMHD snapshots and two EHT2017 images (Wielgus et al. 2020, 11–13). Once tested, this approach was applied to the observational data, resulting in two sets of geometric images, one for each ring model ([figure 10](#)). Having thus created new images of M87*, the researchers moved to translating the images’ figurative spaces into spaces of epistemic action and thus using them to generate novel scientific insights.

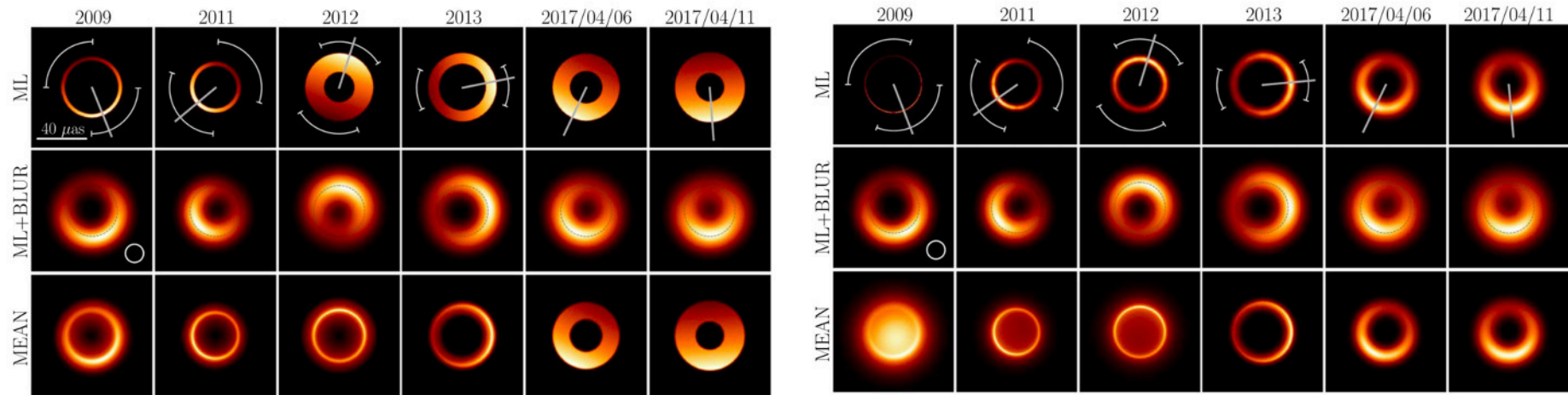


Figure 10. Images of M87* obtained by fitting two ring models to the EHT datasets 2009–17.

Wielgus et al. 2020. <https://creativecommons.org/licenses/by/4.0/>.

As with the initial EHT images, the researchers first identified and then quantified the geometric images’ salient visual features: the ring diameter, orientation of the brightness asymmetry, and central flux depression. The quantification revealed that a central shadow was present in most geometric images, except some of those computed from the pre-2013 data, which had severely limited coverage (Wielgus et al. 2020, 17–18). But the crucial discovery was that the ring diameter in all images from the different epochs was consistent and matched the ring diameter of the EHT2017 total intensity images. Foregrounding this consistency, the researchers declared that the emission ring was a persistent feature of M87*’s morphology (Wielgus et al. 2020, 19). The geometric maps thus fulfilled a significant epistemic function by empirically stabilising the interpretation of the total intensity EHT2017 images as images of a black hole shadow.

Additionally, through contrastive differentiation of the geometric maps from the different epochs, the researchers determined that the position angle of the emission ring’s brightness asymmetry varied from 2009 to 2017, shifting between the south-north and east-west orientations (Wielgus et al. 2020, 19). This discovery had two significant implications. First, it allowed the researchers to distinguish between the ring size as the stable image feature, on the one hand, and “the transient [image] features associated with the turbulent accretion flow,” on the other hand (Wielgus et al. 2020, 19). Second, by quantitatively comparing the geometric images of M87* with the GRMHD simulations created in 2019, the researchers attributed the observed variability in the ring asymmetry to the “intrinsic structural variability” of M87* (Wielgus et al. 2020, 19). The latter comparison also allowed them to constrain the range of GRMHD models that matched their initial EHT images by excluding the models that lacked the temporal variations in the brightness asymmetry displayed by the geometric images. Thus, despite their visual simplicity, the geometric images proved to be productive epistemic tools for mapping M87*’s dynamic features. As I have shown, the geometric images also shifted the interpretation of the EHT2017 images by enabling the differentiation between the stable and the transient visual features and by limiting the range of the viable GRMHD models.

The EHT mapping of M87*’s dynamic features continued in 2021 with the creation and interpretation of polarimetric images. To create this type of image, the researchers revisited their EHT2017 data. But this time, instead of reconstructing the spatial distribution of the radiation intensity emitted by M87* on event-horizon scales, the team aimed to visualise the spatial pattern of the radiation’s linear polarisation. To identify the latter pattern that contains information about the configuration of the accretion flow’s underlying magnetic fields near the event horizon (EHTC 2021b, 1), the researchers submitted the EHT2017 data to a specifically developed algorithmic

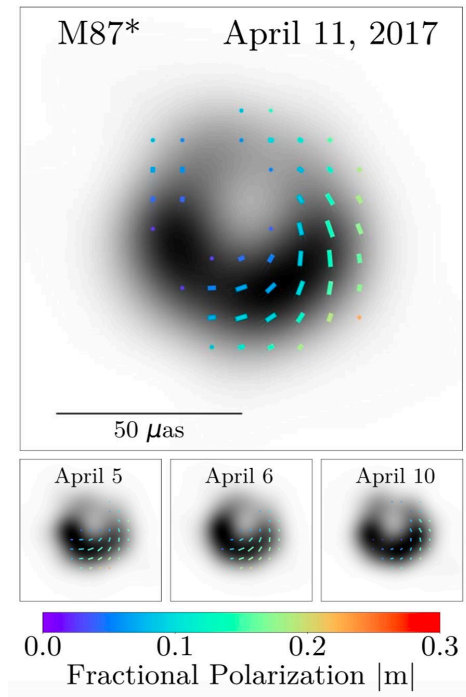


Figure 11. Pipeline-averaged polarimetric images of M87* for four measurement days in April 2017.

EHTC 2021b. <https://creativecommons.org/licenses/by/4.0/>.

processing. Also in this case, the algorithmic processing entailed multiple operations such as correlation, calibration, and the subsequent multistage image reconstruction.

For our discussion, it suffices to mention that during the polarimetric image reconstruction, the researchers deployed five algorithmic pipelines informed by three different modelling approaches (EHTC 2021a, 5–9). To determine the optimal parameters, each algorithm’s performance was tested on six synthetic ground truth polarimetric images derived from GRMHD simulations and simple geometric models. Importantly, while computing the EHT polarimetric images, the researchers deployed a set of the initial fiducial total intensity EHT images to guide the algorithmic process (EHTC 2021a, 7). Thus, the initial EHT images served as a reference for creating the polarimetric images of M87*. Through this process, the researchers obtained twenty fiducial polarimetric images, five for each measurement day (EHTC 2021a, 9). Blurring the images for each day to a common resolution and averaging them across the pipelines, they created the “conservative” visualisations of their final polarimetric imaging results, in which the pipeline-specific idiosyncrasies were attenuated (EHTC 2021a, 10). The polarimetric patterns were visualised using ticks whose varying colours, lengths, and orientations encode the changing amplitudes, intensity, and direction of the linear polarisation. The patterns were then superimposed on the initial EHT total intensity images that were grey-scale coded ([figure 11](#)).

The resulting composite images allowed the researchers to expand their cartographic impulse by exploring the previously inaccessible dynamic aspects of M87*. For example, a consistent visual feature across all the polarimetric images was the azimuthal pattern of linearly polarised emission in the ring’s southwest part. By quantifying the pattern’s geometry, the researchers made inferences about the underlying astrophysical processes that happen in the vicinity of the event horizon. They thus attributed the pattern to “Faraday rotation internal to the emission ring, which acts to rotate, scramble, and depolarise the resolved polarized emission” (EHTC 2021b, 16). Combining this conjecture with the parameters of the EHT2017 images as constraining factors, the researchers could estimate multiple physical properties of the magnetised plasma in M87*’s accretion flow, such as the average density, magnetic field strength, and electron temperature (EHTC 2021b, 4–5).

Next, the researchers quantitatively compared the polarimetric images of M87* to synthetic polarimetric images derived from theoretical models. For this purpose, they used the three-dimensional time-dependent GRMHD simulations of magnetised accretion flows generated in 2019, which comprised either the MAD models with strong magnetic fields that affect the plasma flow dynamics or the opposing SANE models. Using ray-tracing codes, the researchers created seventy-two thousand two-dimensional polarimetric snapshots from one hundred twenty simulated models that covered diverse physical scenarios (EHTC 2021b, 8). The comparison of the polarimetric GRMHD snapshots with the EHT polarimetric images delivered a critical new insight: “Combined with a conservative lower limit on the jet power of M87, only strongly magnetized (MAD) models remain viable” (EHTC 2021b, 23). The researchers then used the remaining MAD models to estimate the black hole’s key dynamic parameter—the yearly mass accretion rate that designates the amount of matter falling into the black hole. But crucially, by eliminating all SANE models as viable interpretations of M87*’s accretion dynamics, the team retrospectively significantly constrained the interpretational ambiguity of the initial EHT images (see [figure 1](#)).

To sum up, this section has outlined how the subsequent images computed from the archival test data and through the polarimetric imaging of the EHT2017 dataset have fulfilled important epistemic functions in the iterative mapping of M87* by delivering context-specific “solutions to relational problems” (Kitchin and Dodge 2007, 342). Specifically created to address the questions the initial EHT images could not, the latter images opened up additional epistemic perspectives on the same research object. The geometric and polarimetric images thus expanded the EHT team’s cartographic impulse by enabling the exploration of previously inaccessible dynamic features of M87*’s accretion flow and its underlying magnetic structure.

My analysis has highlighted that, instead of being mutually exclusive, these different images are not just epistemically complementary but are also closely interlinked through a network of dynamic, multidirectional relations. As discussed above, the EHT2017 images played significant roles in constructing and interpreting the subsequent images. Moreover, the new insights won by interpreting the geometric and polarimetric maps shifted the meaning of the initial total intensity images, constraining their semantic ambiguity. It can, therefore, be said that the iterative and still ongoing mapping of M87* entails the production of chains of EHT images. In this chain, the existing images inform the creation of new images. But just as importantly, new images do not simply displace the existing images or make them redundant but instead add novel layers of meaning to them. The images’ cumulative operative capacity and epistemic efficacy thus increase as the chain of images continues to grow. And although my analysis in this article has focused on how the dynamic, iterative operations that underpin the production and interpretation of continually growing chains of images has been implemented in the EHT mapping of M87*, such epistemic operations are not limited to this particular case study. Instead, insights won through this analysis and the methodological approach developed here have broader implications for our understanding of how images, when used as epistemic tools, are implicated in processes of knowledge production across different areas of scientific research.

Conclusion

After the EHT team announced in April 2019 their historical feat of imaging a black hole—an astrophysical object hitherto thought “unseeable”—most media reports focused on a single EHT image, often erroneously designating it a photograph (Dunham 2019; Strickland 2019). However, drawing on Sybille Krämer, Bruno Latour, and proponents of critical cartography, I have argued that, in the scientific context, it makes little sense to isolate single EHT images or treat them as purportedly straightforward visual depictions of a black hole. Instead, as I have shown in this article, the chains of mutually interconnected EHT images function as epistemic tools that researchers use to actively explore a previously unknown cosmic environment, assess the assumption of it being a Kerr black hole, and infer its physical properties and dynamic behaviour. In the process, researchers are gaining novel empirical insights into the nature of the perhaps most extraordinary astrophysical objects in the universe, testing the predictions of general relativity, and constraining the current theoretical models of black holes. I have also claimed that to understand how and what kinds of scientific insights the EHT images generate and with which epistemic limitations, we must analyse the joint operations that experts perform when creating, reading, and interpreting these images.

My analysis has underscored that the epistemic operativity of the EHT images as tools for mapping the black hole’s environment hinges on two things. First, during various stages of their production and subsequent deployment, the EHT images had to be embedded into suites of synthetic images, theoretical

models, computer simulations, and previous non-EHT measurements. All these external referents served as crucial semantic anchoring points that informed the creation of various EHT images. Moreover, only by relating the EHT images to other purposefully selected images and models could the researchers transform the EHT images’ visually fixed configurative spaces into active spaces of knowledge production, thus activating the cartographic impulse. Consequently, the potential validity of the epistemic gains obtained through this process depends on the adequacy and accuracy of all the elements comprising the thus constructed interpretative framework, which not only enables but, at the same time, also constrains the kinds of insight that can be won with the EHT images. Second, we have seen that each EHT image provides only partial, relational insights into the black hole’s environment. This limited epistemic efficacy of any single image necessitates the iterative production of subsequent images to address the questions the previous images could not. Hence, the images discussed here are part of an unfolding iterative mapping procedure. This mapping will continue to deliver new, less blurry static empirical images and, in the future, also videos of black holes, which when used operatively will expand our knowledge of the universe.

To conclude my analysis, I want to address some broader sociocultural implications of the EHT images of M87* as knowledge-producing tools. As Latour (1987) and Kitchin, Dodge, and Perkins (2011) have argued, in providing access to a territory, maps also invest their users with the symbolic power over this territory, and the EHT images, when used as maps, are no exception. Thus, unsurprisingly, in interviews addressing the general public, their creators have characterised these images as the ultimate tools of epistemic conquest that have reconfigured the boundaries of the knowable, revealing the “majestic mystery of our universe” (Strickland 2019). In slightly utopian terms, some team members have additionally hailed the EHT images as a “moving demonstration of what humanity is capable of” (Dunham 2019). Overall, these images that visualise an invisible black hole not from the Apollonian perspective but from the vantage point of Earth were declared a symbol of the efficacy of collaborative spirit and the pinnacle of human ingenuity.¹⁷ While such interpretative framing gives due credit to the remarkable achievement of this mapping endeavour, it also entails implicit anthropocentric connotations reflected in its emphasis on human epistemic dominance and control over nature.

Finally, I want to point out another aspect of implicit power relations that becomes apparent when the EHT images are approached from an operative perspective. Although they were produced through a collective effort that spanned continents and united scientists from different disciplines, and despite the team’s investment in making the data, imaging algorithms, and findings

¹⁷ For a discussion and criticism of such celebratory framing, see Beier (2021).

publicly available, the EHT images have an unavoidably exclusionary aspect. As detailed in this article, creating and using these images as maps that enable epistemic exploration of the otherwise inaccessible black hole’s environment requires highly specialised expert knowledge and access to sophisticated software and hardware. Thus, the number of people who can actively deploy these images as knowledge-producing tools is very limited. For the rest of us, who lack the expertise and/or access to high-end technological facilities, the EHT images are merely beautiful pictures. This, however, does not diminish the revolutionary nature and the operative efficacy of these images as novel epistemic tools in black hole physics.

Author Biography

Paula Muhr is a postdoctoral researcher at the Institute for History of Art and Architecture, Karlsruhe Institute of Technology (KIT), and a visual artist. She studied visual arts, art history, theory of literature, and physics before receiving her PhD in art and visual history from the Humboldt University Berlin. Her interdisciplinary research is at the intersection of visual studies, image theory, media studies, science and technology studies (STS), medical humanities, and history and philosophy of science. She examines knowledge-producing functions of new imaging and visualisation technologies in natural sciences, ranging from neuroscience over medicine to black hole physics. Since 2022, she has been an active member of the History Philosophy and Culture (HPC) Working Group of the Next Generation Event Horizon Telescope (ngEHT) Collaboration. She recently published her first monograph, *From Photography to fMRI: Epistemic Functions of Images in Medical Research on Hysteria* (transcript, 2022; open access).

Acknowledgements

I would like to thank this theme issue’s guest co-editors, in particular Lila Lee-Morrison, and journal co-editor-in-chief Janet Walker for their helpful suggestions, support, and dedication. I also extend my gratitude to Puragra (Raja) GuhaThakurta for his openness to interdisciplinary dialogue and his insightful comments. Finally, I thank the two anonymous reviewers of this journal for their remarks on an earlier draft of this manuscript.



This is an open-access article distributed under the terms of the Creative Commons Attribution 4.0 International License (CCBY-4.0). View this license’s legal deed at <http://creativecommons.org/licenses/by/4.0> and legal code at <http://creativecommons.org/licenses/by/4.0/legalcode> for more information.

REFERENCES

- Alpaydin, Ethem. 2020. *Introduction to Machine Learning*. 4th ed. Cambridge, MA: MIT Press.
- Beier, Jessie. 2021. “Tracing a Black Hole: Probing Cosmic Darkness in Anthropocenic Times.” In *Reimagining Science Education in the Anthropocene*, edited by Maria Wallace, Jesse Bazzul, Marc Higgins, and Sara Tolbert, 35–52. Cham: Palgrave Macmillan. https://doi.org/10.1007/978-3-030-79622-8_3.
- Bouman, Katherine L. 2017. “Extreme Imaging via Physical Model Inversion: Seeing Around Corners and Imaging Black Holes.” PhD Diss., Massachusetts Institute of Technology.
- . 2020. “Portrait of a Black Hole: Here’s How the Event Horizon Telescope Team Pieced Together a Now-Famous Image.” *IEEE Spectrum* 57 (2): 22–29. <https://doi.org/10.1109/mspec.2020.8976898>.
- Bouman, Katherine L., Michael D. Johnson, Daniel Zoran, Vincent L. Fish, Sheperd S. Doeleman, and William T. Freeman. 2016. “Computational Imaging for VLBI Image Reconstruction.” 2016 *IEEE Conference on Computer Vision and Pattern Recognition (CVPR)*, June. <https://doi.org/10.1109/cvpr.2016.105>.
- Coopmans, Cateljine, Janet Vertesi, Michael Lynch, and Steve Woolgar, eds. 2014. *Representation in Scientific Practice Revisited*. Cambridge, MA: MIT Press. <https://doi.org/10.7551/mitpress/9780262525381.001.0001>.
- Dunham, Will. 2019. “‘Seeing the Unseeable’: Scientists Reveal First Photo of Black Hole.” *Reuters*. <https://www.reuters.com/article/us-space-exploration-blackhole-idUSKCN1RM1OP>.
- Epple, Angelika, and Walter Erhart. 2020. “Practices of Comparing: A New Research Agenda Between Typological and Historical Approaches.” In *Practices of Comparing: Towards a New Understanding of a Fundamental Human Practice*, edited by Angelika Epple, Walter Erhart, and Johannes Grave, 11–38. Bielefeld: transcript. <https://doi.org/10.2307/j.ctv2f9xscg.4>.
- Event Horizon Telescope Collaboration (EHTC). 2019a. “First M87 Event Horizon Telescope Results. I. The Shadow of the Supermassive Black Hole.” *The Astrophysical Journal Letters* 875, L1: 1–17. <https://doi.org/10.3847/2041-8213/ab0ec7>.
- . 2019b. “First M87 Event Horizon Telescope Results. II. Array and Instrumentation.” *The Astrophysical Journal Letters* 875, L2: 1–28. <https://doi.org/10.3847/2041-8213/ab0c96>.
- . 2019c. “First M87 Event Horizon Telescope Results. III. Data Processing and Calibration.” *The Astrophysical Journal Letters* 875, L3: 1–32. <https://doi.org/10.3847/2041-8213/ab0c57>.
- . 2019d. “First M87 Event Horizon Telescope Results. IV. Imaging the Central Supermassive Black Hole.” *The Astrophysical Journal Letters* 875, L4: 1–52. <https://doi.org/10.3847/2041-8213/ab0e85>.
- . 2019e. “First M87 Event Horizon Telescope Results. V. Physical Origin of the Asymmetric Ring.” *The Astrophysical Journal Letters* 875, L5: 1–31. <https://doi.org/10.3847/2041-8213/ab0f43>.
- . 2019f. “First M87 Event Horizon Telescope Results. VI. The Shadow and Mass of the Central Black Hole.” *The Astrophysical Journal Letters* 875, L6: 1–44. <https://doi.org/10.3847/2041-8213/ab1141>.
- . 2021a. “First M87 Event Horizon Telescope Results. VII. Polarization of the Ring.” *The Astrophysical Journal Letters* 910, L12: 1–48. <https://doi.org/10.3847/2041-8213/abe71d>.
- . 2021b. “First M87 Event Horizon Telescope Results. VIII. Magnetic Field Structure near The Event Horizon.” *The Astrophysical Journal Letters* 910, L13: 1–43. <https://doi.org/10.3847/2041-8213/abe4de>.

- Falcke, Heino, Fulvio Melia, and Eric Agol. 2000. “Viewing the Shadow of the Black Hole at the Galactic Center.” *The Astrophysical Journal* 528 (1): L13–16. <https://doi.org/10.1086/312423>.
- Farocki, Harun. 2004. “Phantom Image.” *Public* 29: 12–22.
- Galison, Peter. 2021. “‘Images Scatter into Data, ...’—Iconoclasm and the Scientific Image: Talk with Peter Galison. Online Talk Moderated by Livia Nolasco-Rózsás.” In *BEYOND MATTER? – A Revival of Clashes between Materiality and Representation*. ZKM Center for Art and Media Karlsruhe. <https://youtu.be/feOm6StmwUQ>.
- Goddi, Ciriaco, Geoff Crew, Violette Impellizzeri, Iván Martí-Vidal, Lynn D. Matthews, Hugo Messias, Helge Rottmann, et al. 2019. “First M87 Event Horizon Telescope Results and the Role of ALMA.” *The Messenger* 177: 25–35. <https://doi.org/10.18727/0722-6691/5150>.
- Hoel, A. S. Aurora. 2021. “Image Agents.” *The Nordic Journal of Aesthetics* 30 (61–62): 120–26. <https://doi.org/10.7146/nja.v30i61-62.127889>.
- Hoel, Aud Sissel. 2018. “Operative Images. Inroads to a New Paradigm of Media Theory.” In *Image – Action – Space: Situating the Screen in Visual Practice*, edited by Luisa Feiersinger, Kathrin Friedrich, and Moritz Queisner, 11–27. Berlin: De Gruyter. <https://doi.org/10.1515/9783110464979-002>.
- Jaton, Florian. 2021. “Assessing Biases, Relaxing Moralism: On Ground-Truthing Practices in Machine Learning Design and Application.” *Big Data & Society* 8 (1): 1–15. <https://doi.org/10.1177/20539517211013569>.
- Kitchin, Rob, and Martin Dodge. 2007. “Rethinking Maps.” *Progress in Human Geography* 31 (3): 331–44. <https://doi.org/10.1177/0309132507077082>.
- Kitchin, Rob, Martin Dodge, and Chris Perkins. 2011. “Introductory Essay: Power and Politics of Mapping.” In *The Map Reader: Theories of Mapping Practice and Cartographic Representation*, edited by Martin Dodge, Rob Kitchin, and Chris Perkins, 387–94. Chichester: Wiley-Blackwell. <https://doi.org/10.1002/9780470979587.ch50>.
- Kitchin, Rob, Chris Perkins, and Martin Dodge. 2011. “Thinking about Maps.” In *Rethinking Maps: New Frontiers in Cartographic Theory*, edited by Martin Dodge, Rob Kitchin, and Chris Perkins, 1–25. New York: Routledge.
- Krämer, Sybille. 2009. “Operative Bildlichkeit. Von der ‘Grammatologie’ zu einer ‘Diagrammatologie’? Reflexionen über erkennendes ‘Sehen.’” In *Logik des Bildlichen: zur Kritik der ikonischen Vernunft*, edited by Martina Heßler and Dieter Mersch, 94–122. Bielefeld: transcript. <https://doi.org/10.1515/9783839410516-003>.
- . 2011. “‘The Mind’s Eye’: Visualizing the Non-Visual and the ‘Epistemology of the Line.’” In *Image and Imaging in Philosophy, Science and the Arts*, edited by Richard Heinrich, Elisabeth Nemeth, Wolfram Pichler, and David Wagner, 2:275–93. Frankfurt: Ontos.
- . 2015. *Medium, Messenger, Transmission: An Approach to Media Philosophy*. Translated by Anthony Enns. Amsterdam: Amsterdam University Press.
- . 2018. “‘Kartographischer Impuls’ und ‘operative Bildlichkeit’: Eine Reflexion über Karten und die Bedeutung räumlicher Orientierung beim Erkennen.” *Zeitschrift für Kulturwissenschaften* 12 (1): 19–32. <https://doi.org/10.14361/zfk-2018-120105>.
- . 2021. “From Dissemination to Digitality: How to Reflect on Media.” *Media Theory* 5 (2): 79–98.
- Latour, Bruno. 1987. *Science In Action: How to Follow Scientists and Engineers through Society*. Cambridge, MA: Harvard University Press.
- . 1999. *Pandora’s Hope: Essays on the Reality of Science Studies*. Cambridge, MA: Harvard University Press.

- Ljungberg, Christina. 2016. “The Diagrammatic Nature of Maps.” In *Thinking with Diagrams: The Semiotic Basis of Human Cognition*, edited by Sybille Krämer and Christina Ljungberg, 139–59. Berlin: De Gruyter. <https://doi.org/10.1515/9781501503757-007>.
- Macrobert, Alan. 2017. “How to Use a Star Chart with a Telescope.” Sky & Telescope. March 4, 2017. <https://skyandtelescope.org/astronomy-resources/using-a-map-at-the-telescope/>.
- Mende, Doreen, and Tom Holert. 2019. “Editorial: Navigation Beyond Vision.” E-flux journal 101. 2019. <https://www.e-flux.com/journal/101/274019/editorial-navigation-beyond-vision-issue-one/>.
- Mizuno, Yosuke. 2022. “GRMHD Simulations and Modeling for Jet Formation and Acceleration Region in AGNs.” *Universe* 8 (2): 85. <https://doi.org/10.3390/universe8020085>.
- Morrison, Margaret. 2015. *Reconstructing Reality: Models, Mathematics, and Simulations*. Oxford, New York: Oxford University Press. <https://doi.org/10.1093/acprof:oso/9780199380275.001.0001>.
- Muhr, Paula. 2024. “‘What We Thought Was Unseeable’: Die Konstruktion des authentischen Bildes eines Schwarzen Lochs.” In *‘Ain’t Nothing Like the Real Thing?’: Formen und Funktionen medialer Artefakt-Authentifizierung*, edited by Amrei Bahr and Gerrit Fröhlich. Bielefeld: transcript.
- . Forthcoming. “Establishing Trust in Algorithmic Results: Ground Truth Simulations and the First Empirical Images of a Black Hole.” In *The Science and Art of Simulation: Trust in Science*, edited by Nico Formánek, Ammu Joshy, and Andreas Kaminski. Cham: Springer.
- November, Valérie, Eduardo Camacho-Hübner, and Bruno Latour. 2010. “Entering a Risky Territory: Space in the Age of Digital Navigation.” *Environment and Planning D: Society and Space* 28 (4): 581–99. <https://doi.org/10.1068/d10409>.
- Parikka, Jussi. 2023. *Operationa Images: From the Visual to the Invisual*. Minneapolis: University of Minnesota Press. <https://doi.org/10.5749/9781452970929>.
- Siegert, Bernhard. 2011. “The Map Is the Territory.” *Radical Philosophy* 169 (5): 13–16. <https://doi.org/10.25969/MEDIAREP/13157>.
- Skulberg, A.E.G. 2021. “The Event Horizon as a Vanishing Point: A History of a First Image of a Black Hole Shadow from Observation.” PhD Diss., University of Cambridge.
- Strickland, Ashley. 2019. “This Is the First Photo of a Black Hole.” CNN. April 10, 2019. <https://edition.cnn.com/2019/04/10/world/black-hole-photo-scn/index.html>.
- Thompson, A.Richard, James M. Moran, and George W. Swenson. 2017. *Interferometry and Synthesis in Radioastronomy*. 3rd ed. Cham: Springer.
- Vertesi, Janet. 2015. *Seeing Like a Rover: How Robots, Teams, and Images Craft Knowledge of Mars*. Chicago: University of Chicago Press. <https://doi.org/10.7208/chicago/9780226156019.001.0001>.
- Wielgus, Maciek, Kazunori Akiyama, Lindy Blackburn, Chi-kwan Chan, Jason Dexter, Sheperd S. Doleman, Vincent Fish, et al. 2020. “Monitoring the Morphology of M87 in 2009–2017 with the Event Horizon Telescope.” *The Astrophysical Journal* 901 (67): 1–28. <https://doi.org/10.3847/1538-4357/abac0d>.